Neurol Med Chir (Tokyo) 54, 775–785, 2014
doi: 10.2176/nmc.st.2014-0176
Online September 29, 2014

The 72nd Annual Meeting Special Topic:
Neurosurgery in Update

Novel Techniques of Real-time Blood Flow and Functional Mapping: Technical Note

Kyousuke KAMADA,[1] Hiroshi OGAWA,[1] Masato SAITO,[1] Yukie TAMURA,[1] Ryogo ANEI,[1] Christoph KAPELLER,[2] Hideaki HAYASHI,[3] Robert PRUECKL,[2] and Christoph GUGER[2]

[1]*Department of Neurosurgery, School of Medicine, Asahikawa Medical University, Asahikawa, Hokkaido;*
[2]*Technical Development Division, Guger Technologies OG, Graz, Austria;*
[3]*Technical Development Division, Infocom, Tokyo*

Abstract

There are two main approaches to intraoperative monitoring in neurosurgery. One approach is related to fluorescent phenomena and the other is related to oscillatory neuronal activity. We developed novel techniques to visualize blood flow (BF) conditions in real time, based on indocyanine green videography (ICG-VG) and the electrophysiological phenomenon of high gamma activity (HGA). We investigated the use of ICG-VG in four patients with moyamoya disease and two with arteriovenous malformation (AVM), and we investigated the use of real-time HGA mapping in four patients with brain tumors who underwent lesion resection with awake craniotomy. Real-time data processing of ICG-VG was based on perfusion imaging, which generated parameters including arrival time (AT), mean transit time (MTT), and BF of brain surface vessels. During awake craniotomy, we analyzed the frequency components of brain oscillation and performed real-time HGA mapping to identify functional areas. Processed results were projected on a wireless monitor linked to the operating microscope. After revascularization for moyamoya disease, AT and BF were significantly shortened and increased, respectively, suggesting hyperperfusion. Real-time fusion images on the wireless monitor provided anatomical, BF, and functional information simultaneously, and allowed the resection of AVMs under the microscope. Real-time HGA mapping during awake craniotomy rapidly indicated the eloquent areas of motor and language function and significantly shortened the operation time. These novel techniques, which we introduced might improve the reliability of intraoperative monitoring and enable the development of rational and objective surgical strategies.

Key words: arrival time, awake craniotomy, blood flow, fluorescence, high gamma activity

Introduction

Digital data processing has become faster in recent years because of advancements in both hardware and software. For intraoperative monitoring (IOM) in neurosurgery, there are two main approaches to observing brain signals, one based on fluorescent phenomena, and the other based on oscillatory neuronal activity. Using digital data processing, essential information on both types of signal can be visualized during neurosurgical operations. Electronic engineering has become increasingly important in medical practice, and neurosurgeons who wish to make use of recently developed and highly technical devices must understand the basics of the electronics involved to master the intraoperative use of these new devices and techniques.

Although IOM has been used in clinical practice for approximately 20 years, there is still no consensus

Received May 12, 2014; Accepted July 2, 2014

on the efficacy of cortical mapping in preventing postoperative neurological deficits. Cortical somatosensory evoked potentials (SEPs) monitor only the sensory functions and areas supplied by the middle cerebral artery. Motor functions can be monitored by recording muscle responses to electrocortical stimulation (ECS) of the primary motor cortex. However, it is still difficult to monitor language-related functions, and ischemic complications can disrupt IOM.

Recently, fluorescent activity has been used to monitor surgical procedures, including neurosurgery. Indocyanine green (ICG) is a water-soluble, tricarbocyanine, near-infrared fluorescent dye, which was clinically introduced for the measurement of cardiac output in 1969.[1] In plasma, ICG absorbs light at 800 nm and emits light at 835 nm where there is minimal interference from oxy- and deoxy-hemoglobin. Modern neurosurgical microscopes have light sources that deliver light including the ICG excitation wavelength, and they are equipped with optical filters that allow only fluorescence in the ICG emission wavelength. Using these microscopes, surgeons can visualize and record fluorescent images in real time.[2] Intraoperative ICG videography (ICG-VG) is used in vascular neurosurgery to evaluate clip positions and ensure complete occlusion of aneurysms and patency of extracranial-intracranial (EC-IC) bypass. Blood flow (BF) monitoring using ICG-VG has potential for stable IOM in neurosurgery. Another technique based on ICG-VG is also widely used to detect technical failures in coronary bypass grafts; in this setting it is known as intraoperative laser angiography or fluorescence imaging.[3,4] One limitation of this technique at present is that it provides only qualitative results based on 8-bit gray-scale images; quantitative results are not available. Furthermore, in all commercially available systems, ICG-VG can only be viewed on a separate monitor in two dimensions, without depth perception. Therefore, neurosurgeons must optimize the desired view prior to ICG injection, and the operative field must be clear of debris and blood products for the target structures to be visualized.

Another topic regarding IOM in neurosurgery is the need to identify and monitor language-related functions. Several groups have proposed that ECS during awake craniotomy is a reliable way to perform language mapping.[5,6] However, there are technical difficulties involved with this method, including the risk of seizure, need to identify optimal stimulation sites, and symptoms induced by the procedure itself. Power changes in oscillatory neuronal activity within various frequency ranges on electrocorticogram (ECoG) have recently been proposed as potential neurophysiological indicators. Among these oscillatory changes, augmentation of high gamma activity (HGA) ranging from approximately 60 to 140 Hz is assumed to reflect localized cortical processing. Crone et al. constructed HGA maps that indicated language-related functions from patients performing word reading (WR) tasks.[7] Therefore, HGA might provide a key signal for creating accurate brain maps. Based on this information, we proposed that HGA mapping could be a new less-invasive procedure that would shorten the time needed to perform cortical mapping during awake craniotomy.

In the present article, we introduce novel techniques that we have recently developed for the quantitative analysis of ICG-VG and real-time HGA mapping, describe the clinical impact of these techniques, and provide representative cases.

Subjects and Methods

I. Patients

Four patients with moyamoya disease and two patients with arteriovenous malformation (AVM) underwent direct revascularization (EC-IC bypass) and nidus removal. During the operations, we monitored BF conditions using ICG-VG. Four patients with an intra-axial tumor in the left frontotemporal region underwent lesion resection with awake craniotomy and real-time HGA mapping. This study was approved by the institutional review board (No. 693), and written informed consent was obtained from each patient before participation in the study.

II. Methods

1. Quantitative analysis of ICG-VG

Administration of ICG and fluorescent signal measurement: After completing EC-IC bypass, graft patency was assessed using noninvasive techniques such as micro-Doppler ultrasonography and transit time ultrasound flowmetry (HT-300; Transonic Systems Inc., Ithaca, New York, USA) with probes of 1.5 mm, 2.0 mm, and 2.5 mm in diameter. Intraoperative ICG-VG was recorded using a surgical microscope (OH4; Leica Microsystems, Heerbrugg, Switzerland) equipped with a 300-W excitation light source, fluorescence filters, and a data storage server (HDMD; Leica Microsystems, Heerbrugg, Switzerland). A magnification of 2× and a working distance of 200 cm were fixed manually for consistent data acquisition. After setting up the system, 2 ml of ICG solution (25 mg dissolved in 10 ml of water) was injected, and the operative field was illuminated by the light source with a wavelength including part of the ICG absorption band. The fluorescence from ICG was recorded using a nonintensified video camera

with optical filters to block ambient light, so only ICG-induced fluorescence was recorded over a range of 780–950 nm. This allowed real-time visualization of arterial, capillary, and venous angiographic phases of flow with excellent resolution. Video clips were recorded on the storage server.

2. Real-time quantitative ICG-VG analysis

Image processing was performed using the real-time ICG analysis software FlowInsight, developed by our group (Infocom, Tokyo). The software operates with dual-boot Linux on a 13-inch Macbook Pro (Apple Computer Inc., Cupertino, California, USA) and automatically copies the ICG-VE video clips from HDMD via Ethernet. Because ICG intensity changes over time, we applied perfusion-based data processing for real-time ICG data analysis. When the main region of interest (ROI) was placed on the graft, the software automatically generated the time density curve (TDC). On TDC, we had to manually select a time interval for the first ICG circulation. Following this process, eight parametric maps were obtained, reflecting the perfusion status. Arrival time (AT) and Grad indicated the duration between ICG injection and the time point when the intensity reached 5% of the maximum peak, and the intensity gradient between AT and the peak time point, respectively. Time-to-peak (TTP) was the duration between ICG injection and the peak time point, whereas blood flow (BV) and mean transit time (MTT) were the intensity-integration between AT and the end point of the first circulation and a mean time point of BV, respectively. Because BF was defined as the blood volume moving through a given volume of brain per unit time, it was obtained by dividing BV by MTT (Fig. 1). Estimated BF could be corrected by the compensation coefficient (kCBF) for each measurement, in comparison with BF measured by transit time ultrasound flowmetry.

Fusion of ICG video clips and parametric maps: We applied the original ICG-VE video clips to parameter maps to emphasize time–domain information. Consequently, each pixel showed multiple parameters depending on ICG-intensity dynamics, generating color-coded video clips. Furthermore, we superimposed the color-coded video clips on anatomical structures under natural light.

Wireless monitor for real-time fusion of ICG and natural light images: A 5-inch monitor was fixed just below the eyepieces of the operating microscope. The monitor displayed all processed data and the fused ICG and natural light images. The fusion process was performed in real time by a multi-format video switcher (V-800HD; Roland Inc., Los Angeles, California, USA). The processed images were transmitted from the switcher to the 5-inch wireless monitor via a wireless extender (HDMI WH01; SoftBank Inc., Tokyo) (Fig. 2).

3. Real-time HGA mapping

ECoG recording during awake craniotomy: All patients underwent ECoG recordings before lesion resection in the awake state. We used two 20-channel ECoG grids and a 4-channel electrode strip with a 3-mm channel diameter and a 10-mm interelectrode distance

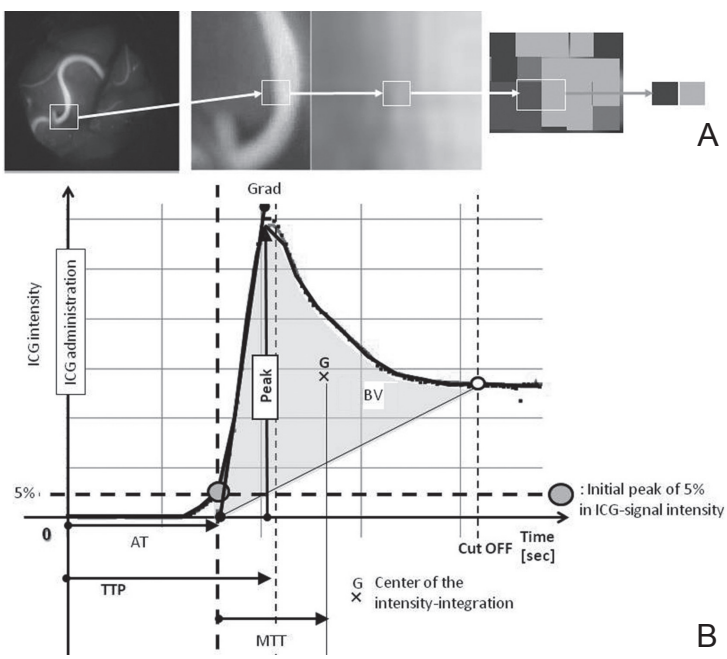

Fig. 1 Intraoperative indocyanine green videography (ICG-VG). A: ICG-VG comprising approximately 400,000 (480 × 640) pixels with 8-bit resolution. B: Time density curve (TDC) of a pixel showing intensity dynamics over time. AT, MTT, BV, TTP, ICG, and G indicate arrival time, mean transit time, blood volume, time to peak, indocyanine green, and the center of BV, respectively. Grad indicates intensity change between AT and the peak point. AT: arrival time, BV: blood flow, ICG: Indocyanine green, MTT: mean transit time, TTP: Time-to-peak.

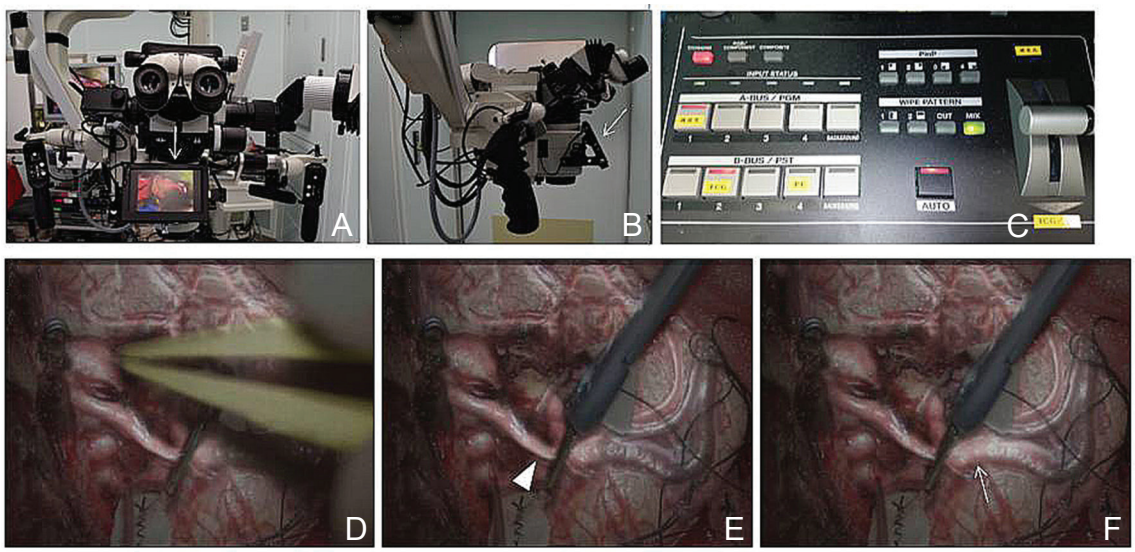

Fig. 2 Wireless monitor fixed just below the eyepieces displaying various images via a wireless extender. A, B: Anterior view (A) and (B) lateral view. Arrows indicate the visual axes of the operator. C: Multi-format video switcher creating fused scenes of indocyanine green (ICG) and natural light images in real time. D: A fused image showing enhancement of a venous pouch by ICG accumulation because of insufficient occlusion of feeders. E: A fused image showing ICG accumulation (*arrowhead*) in a main drainage vein temporally occluded. F: A fused image demonstrating that ICG bulk was moving (*arrow*) after the drainage vein was released.

(Unique Medical Inc., Tokyo). The electrodes were placed on the exposed brain and the positions were registered by a neuronavigation system. The channels of the electrode strip were used as a reference and a ground. The electrode configuration was captured by a digital camera before tumor resection. The ECoG data were recorded at a 1,200-Hz sampling rate using a g.HIamp biosignal amplifier (Guger Technologies OG, Graz, Austria). The data was stored at a 12-bit resolution with a high oversampling ratio, to increase the signal-to-noise ratio.

For the intraoperative ECoG recordings, each patient was first asked to relax for a 20-s baseline period, and then asked to perform a hand grasping (HG) task for 20 s (active period). The baseline and active periods were repeated alternately three times, resulting in a total of 2 min of ECoG measurement (Fig. 3A, B). Patients then performed moving mouth, HG, WR, and picture naming (PN) tasks. A portable monitor was connected to the computer and placed 30 cm ahead of the patient's head. Visual stimuli were presented on the monitor using a real-time processing system driven by the data acquisition computer connected to the g.HIamp. For the WR task, the patient read aloud Japanese words that were presented for 2,000 ms, separated by 500-ms interstimulus intervals. For the PN task, the patients verbally named displayed objects. To obtain a baseline ECoG, the patients passively viewed destructured words or pictures that were presented with the same luminance as the stimuli presented in the active periods.

We developed software dedicated to real-time HGA mapping, named CortiQ, which runs on MATLAB R2012a (Mathworks Inc., Novi, Michigan, USA). After channels containing singular noises were excluded, the software performs a common average reference to suppress common mode signals and calculates the baseline ECoG activity of each channel in the gamma frequency range of 80–120 Hz. The patient is then instructed to perform a specific task, and the software analyzes the ECoG activity during the task. To obtain power averages across HGA, we standardized the power spectral density values with respect to 20 s × 3-ECoG data epochs that included the baseline and active periods (Fig. 3C). A t-test was used to determine whether HGA values in the active periods were significantly different from those in the baseline periods. P values of < 0.05 were considered statistically significant. Bonferroni correction was used to account for the number of electrodes. Finally, the results were visualized in real time in the MATLAB environment as red bubbles, overlaying the electrodes from which the data were recorded, representing significant differences in HGA between the baseline and active periods (Fig. 3D). The significance value was represented by the diameter of the bubble. Computations were

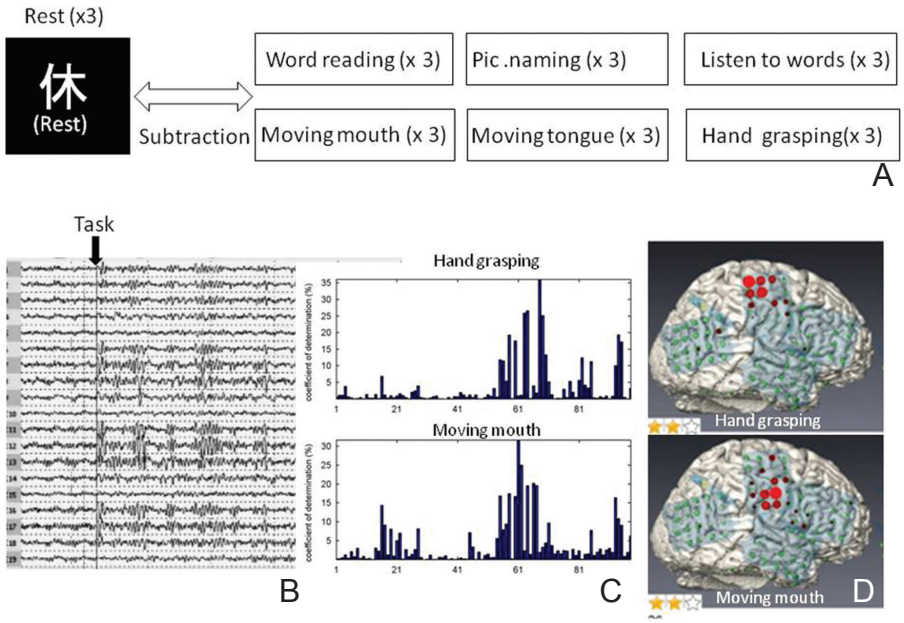

Fig. 3 Overview of high gamma activity (HGA) mapping. A: Experimental designs containing different motor and semantic tasks. B: Intraoperative electrocorticogram of the hand grasping (HG) task showing desynchronization of alpha components at initial onset of the movement. C: Graphs of power changes in HGA of all electrodes demonstrating that active electrodes were different depending on the tasks. D: Real-time HGA mapping of the HG (*upper*) and moving mouth (*lower*) tasks showing significant HGA increases (*red bubbles*) in the primary motor cortex.

performed in real time and updated at 20 Hz.

ECS mapping

After ECoG recording, biphasic electrical pulses (frequency, 50 Hz; pulse duration, 1 ms) were applied to the cortical areas of awake patients (Neuromaster, Nihon Koden Inc., Tokyo) using a bipolar electrode with a 10-mm tip distance (Ojemann cortical stimulator). First, motor mapping was performed to determine the appropriate stimulus intensity at the primary hand motor cortex. Once the threshold was determined for motor mapping, the same stimulus intensity was used for language mapping. We systematically used spontaneous speech, WR, and PN. The key sites, which produced neurological deficits on ECS, were marked with sterilized tags.

Results

I. Quantitative analysis of ICG-VG

Fluorescent signals appeared in the grafts and recipient arteries on the brain surface within 60 s of bolus ICG injection to confirm patency of the bypass grafts (Fig. 4A). The post bypass TDC demonstrated increased intensity and shortened AT and MTT. In the four patients with moyamoya disease, BFs measured by transit time ultrasound flowmetry were 18.5 ml/min, 20.5 ml/min, 26.2 ml/min, and 28.4 ml/min, whereas the respective BFs estimated using FlowInsight were 17.0 ml/min, 19.5 ml/min, 25.5 ml/min, and 26.5 ml/min. kCBF of the compensation coefficient was 0.002 in

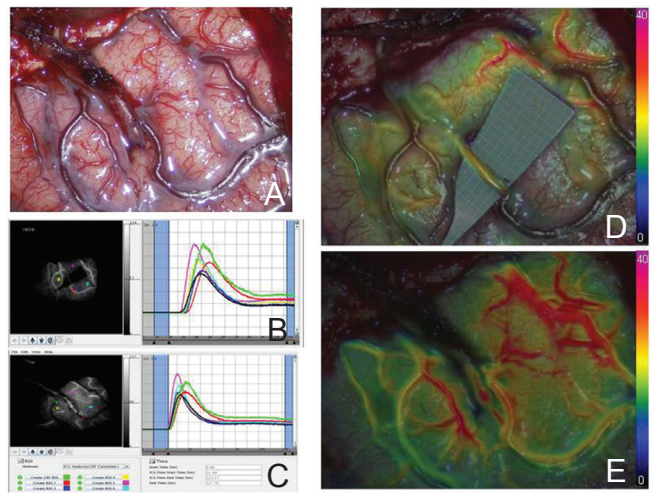

Fig. 4 Revascularization by extracranial-intracranial bypass. A: Operative view under natural light. B: Time density curves (TDCs) before bypass. C: TDCs after revascularization demonstrating markedly shortened arrival time and time to peak. D: Blood flow (BF) map before bypass. E: BF map after revascularization showing BF is increased from 15 ml/min to > 25 ml/min in the graft and recipient areas.

all cases with the fixed conditions. Because ICG injections were performed by anestheologists in a standardized manner, parameters were not affected by the procedure.

We observed estimated BFs of > 25 ml/min on the graft and brain surface vessels (Fig. 4), and AT of the vessels was shortened by 50% (Fig. 5A, B) in two patients after revascularization. These

findings strongly suggested a risk of hyperperfusion syndrome. Patient 4 suffered from a focal seizure in the right of his mouth, and transient aphasia. Postoperative single photon computed tomography (CT) revealed hyperperfusion in the recipient cortical region of the left frontal lobe (Fig. 5C, D). Grafts in the other three patients were patent, and AT, MTT, and TTP were shortened < 10%, and none of the three patients demonstrated hyperperfusion syndrome.

II. Wireless monitor for real-time fusion of ICG and natural light images

The wireless monitor was fixed to the microscope tube in a metal frame. Surgeons could see all the processed images on the monitor via the wireless extender. In addition, real-time fusion images displayed BF and anatomical structures simultaneously (Fig. 2D–F). This enabled us to operate and manipulate vessels on the fusion images, by changing visual axes between the eyepieces and the monitor. It was possible to visualize fusion images as well as other processed images displaying AT, BF, and MTT by using ICG-VG and HGA mapping.

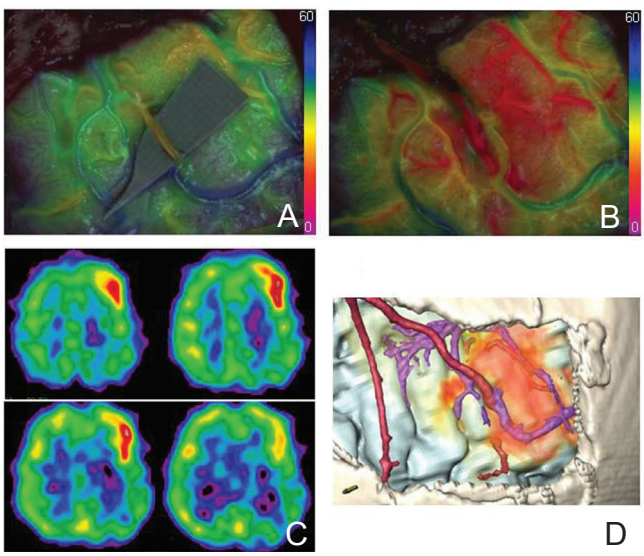

Fig. 5 Revascularization by extracranial-intracranial bypass. A: Arrival time (AT) map before bypass, B: AT map after revascularization showing AT is significantly shortened, suggesting hyperperfusion in the anterior part of the frontal cortex. C: Single photon emission computed tomography (CT) with (99 m) Tc-hexamethylpropylene amine oxime (Tc-HMPAO) delineating hyperperfusion in the left hemisphere. D: three-dimensional (3D)-reconstructed fusion images of 3D CT angiography, anatomical MRI, and (99 m) Tc-HMPAO demonstrating the similar hyperperfusion territory with the AT map.

III. Real-time HGA mapping

All four patients showed minimal impairment of language function. They practiced motor and language tasks before the operation, and after the operation, all patients could read words and name pictures at > 85% of the pre-operation performance rate for all tasks.

After performing the craniotomy, we confirmed that the patient was awake by observing the patient's responses and the bispectral index. We then placed the subdural grids directly on the exposed brain and asked the patient to perform tasks to monitor functions of interest. All patients performed all tasks twice to confirm reproducibility of measurements. ECoG analysis of the HG task (HG-ECoG) demonstrated significant HGA increases in two or three channels that corresponded to the hand motor area. In contrast, PN-ECoG revealed only active channels that corresponded to the inferior frontal gyrus (IFG) or the middle frontal gyrus (MFG) (PN-HGA), but no HGA increase in other frontal regions. Increased HGA on WR-ECoG (WR-HGA) was observed on the same electrodes as PN-HGA on the frontal lobe.

In patient 2, two electrodes (channels M11 and M16, Fig. 6B) of HG-HGA clearly indicated the hand motor area. WR-HGA appeared in four channels (channels F4, F5, F14, and F15, Fig. 6C) on IFG, suggesting that the exposed cortex that included the tumor did not mediate language functions. ECS applied to the localized HG-HGA area initially showed hand muscle contractions. We, then applied ECS to the HGA-positive electrode in the suspected frontal language and confirmed suppression of language related functions (Fig. 6). Sensitivity and specificity of HG and WR-HGA mapping were 100% and 100% compared to ECS mapping, respectively.

In patient 4, WR-fMRI activation appeared wider than WR-HGA. The WR-HGA dynamics demonstrated long-term WR-HGA only in channels F4, F5, F14, and F15 (Fig. 7D) on the frontal lobe. This finding was in contrast to the short-term HGA observed in several channels on the perisylvian region. HGA mapping of patient 4 suggested that changes in PN-HGA and WR-HGA electrodes in MFG were highly related to language function (Fig. 7). In the ECoG analysis, we observed HGA dynamics evoked by language-related tasks in all patients. PN-HGA was visible approximately 10 s into the first active period on channels on the superior temporal gyrus, but immediately diminished. The frontal region showed longer PN-HGA activation. We found similar results in the WR-HGA analysis, which demonstrated that long-term semantic HGA persisted only on the frontal lobe. The neuronavigation system indicated

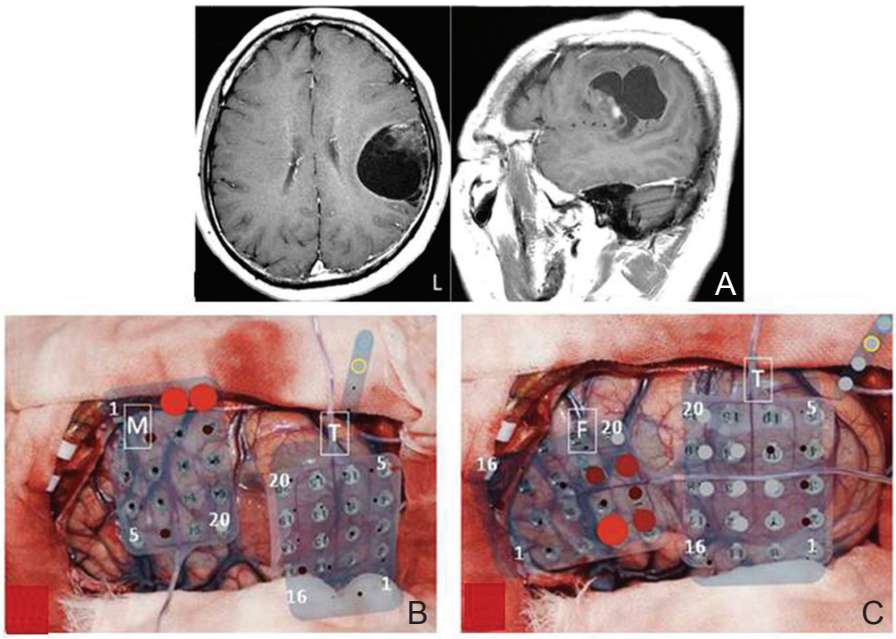

Fig. 6 A: Preoperative contrast-enhanced T_1-weighted magnetic resonance (MR) images of patient 2 showing a lesion with ring-like enhancement in the left frontal lobe. B: Real-time high gamma activity (HGA) mapping by HG task showing significant HGA increase (*red circles* of M11 and 16) in the primary motor cortex. C: Real-time HGA mapping by word reading (WR) task showing significant HGA increase (*red circles* of F4, 5, 14, 15) in the inferior frontal gyrus. Electrocortical stimulation (ECS) to the HGA-positive electrodes consistently evoked hand muscle cramp and language-related symptoms, respectively.

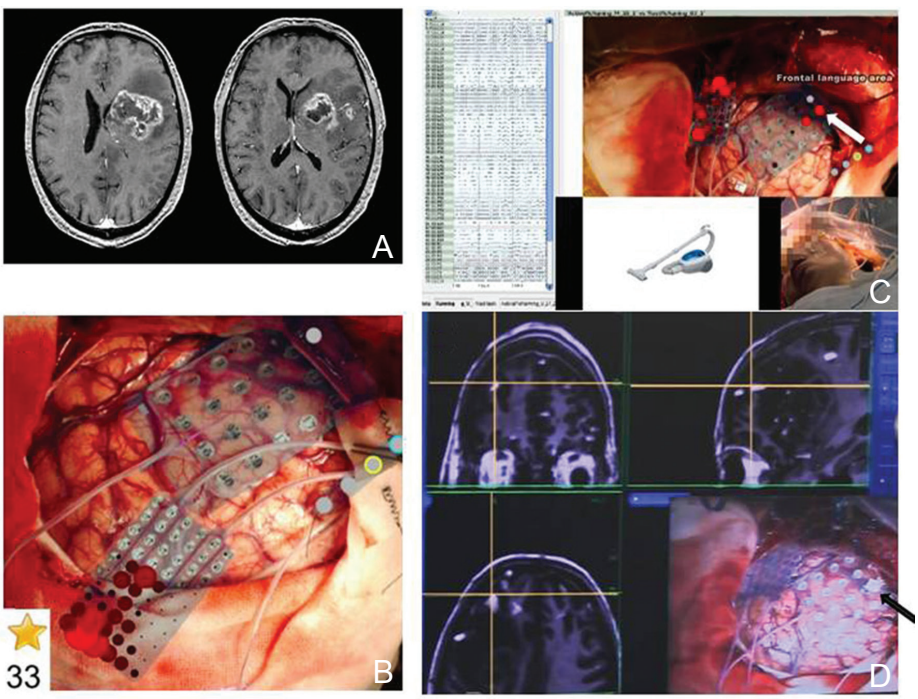

Fig. 7 A: Preoperative contrast-enhanced T_1-weighted magnetic resonance (MR) images of patient 4 showing a lesion with ring-like enhancement in the left frontal lobe with peritumoral edema. B: Real-time high gamma activity (HGA) mapping of the hand grasping task showing a significant HGA increase in the primary hand motor cortex. C: Real-time HGA mapping of the picture naming task showing a significant HGA increase in the temporal lobe and two red bubbles in the middle frontal lobe. D: HGA-positive electrodes on the middle frontal gyrus on the neuronavigation system indicating anteiorshift by the tumor.

HGA-positive electrodes on the frotnal cottex, which was shifted by the tumor.

ECS with 5 mA of stimulus intensity applied to the HG-HGA areas evoked muscle contractions in the right hand (Fig. 7), whereas ECS applied to the PN-HGA areas caused epileptic seizure for a few minutes with afterdischarge. After HGA and ECS mapping, we resected the lesion with a small corticotomy on the posterior part of MFG, preserving motor and language function. After tumor resection, we confirmed that there were no neurological symptoms and that HGA dynamics were unchanged. Patient 4 suffered from transient motor-dominant aphasia and right hemiparesis for a week after the operation. ECS to the PN-HGA and WR-HGA areas consistently evoked speech arrest or naming difficulty in the other three patients. During ECS mapping, we frequently encountered partial

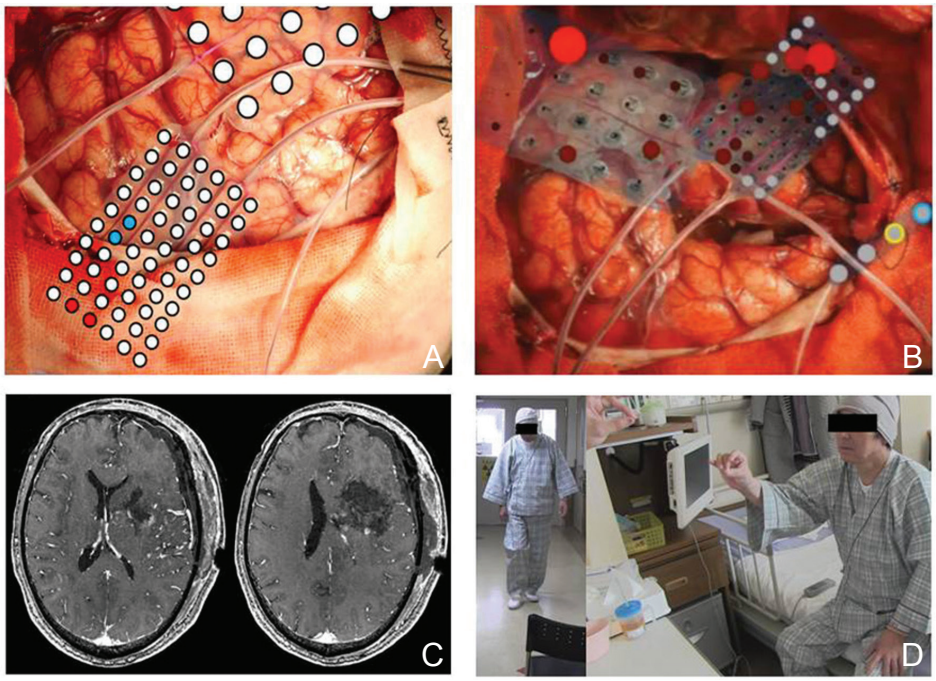

Fig. 8 A: Results of electrocortical stimulation validating the primary hand motor cortex (*red circles*) and inducing epileptic seizure (*blue circles*). B: Real-time high gamma activity (HGA) mapping of the picture naming task after resection showing that the HGA distribution remained the same. C: Postoperative contrast-enhanced T_1-weighted magnetic resonance (MR) images showing gross total removal of the tumor. D: The patient showing no new neurological deficits after tumor resection.

seizures that persisted for several minutes, and in all cases it took quite a few minutes to suppress the seizures (Fig. 8).

Mean times for ECS and HGA mapping were 51.5 ± 11 min and 25.5 ± 5.5 min, respectively. Compared to HGA mapping, ECS mapping took a significantly longer time ($P < 0.01$), because we needed to determine appropriate stimulation intensities and control epileptic seizures. Real-time HGA mapping revealed functional distributions in all patients for both the exposed cortex and hidden regions because of dura matter adhesion. In conclusion, real-time HGA mapping matched the ECS results, and this technique has potential application for predicting the location of eloquent areas.

Discussion

In this study, we have introduced new techniques for real-time data processing of BF and brain signal oscillations in neurosurgery. The software FlowInsight performs real-time data processing of ICG-VG based on perfusion imaging. The present study results demonstrated that changes in several parameters, including AT, MTT, BV, and BF, during an operation could suggest a risk of hyperperfusion. In addition, estimated BF has the potential to indicate the real BF measured by ultrasound flowmetry. Real-time fusion images on the wireless monitor enabled us to manipulate vessels under the microscope without interruption, thereby providing anatomical and BF information simultaneously. For the analysis of brain signal oscillation, we focused on HGA measured using cortiQ and succeeded in conducting real-time HGA mapping during awake craniotomy. Real-time HGA mapping rapidly indicated the eloquent areas of motor and language function and significantly shortened the operation time. We believe that the combination of these techniques increases the reliability of IOM, and enables the development of rational and objective operation strategies.

Because all the medical data is digitally stored, post-acquisition processing is performed based on a digital sampling system. In addition, the characteristic profiles of the particular frequency bands of imaging and electrophysiology can be taken into account, depending on physiological targets of interest. It would be beneficial for physicians, including neurosurgeons, to understand the basics of medical data structures, including the Nyquist sampling theorem and fluorescence phenomena, and apply new techniques for clinical practice. ICG is used as a marker in the assessment of the perfusion of tissues in many medical fields.[8,9] In the past, dye dilution with ICG was a widely used technique for measuring cardiac output.[10] ICG was injected directly through a catheter, usually into the pulmonary artery. Blood was sampled from a second catheter placed in the femoral or brachial artery, and the dye concentration in the sampled blood was measured. In 1990, the 805-nm blood oximeter was developed for measuring TDC of ICG, and the first

passage of ICG circulation was thought to exactly reflect BF. However, the thermodilution technique replaced this method because it was easier to use. In 1995, spiral data acquisition using multi-detector CT scanners enabled users to obtain dynamic perfusion CT, based on a concept similar to the dye dilution technique. Several groups have compared quantitative cerebral BF measurements using CT perfusion with measurements using $H_2{}^{15}O$ positron emission tomography (PET).[11,12] Results of those studies showed that cerebral BF values derived from CT perfusion had a tendency toward overestimation compared with those from PET. The principles of BF measurement are not identical between CT and PET. Cerebral BF measurements with $H_2{}^{15}O$ PET use a diffusible tracer, and tissue perfusion can be measured directly. Because the iodinated contrast material used in dynamic CT perfusion imaging acts as a nondiffusible intravascular tracer, absolute tissue perfusion cannot be measured directly. Instead, intravascular BF is measured. In contrast, various perfusion imaging techniques have been reported efficient for the clinical investigation of acute stroke patients.[13] Although there is no doubt that impaired BF below a certain critical level is the primary cause for functional and structural neuronal damage, various perfusion-related parameters have been proposed to describe cerebral ischemia with respect to the extent and severity of ischemic conditions by comparing them to the unaffected side.

In the present study, we used BF measured by transit time ultrasound flowmetry and ICG-VE. The first transit time flowmetry was described by Plass.[14] Transit time flowmetry is theoretically independent of the internal or external vessel diameter, vessel shape, and BF profile. The probe does not have to be in direct contact with the vessel wall, but an acoustic fluid (gel or blood) must be present between the blood vessel and the probe to ensure good acoustic coupling. The volume flow measurement is independent of the hematocrit fraction, heart rate, and thickness of the vessel wall and is therefore stable and reliable.[15,16] ICG is a nondiffusible intravascular tracer, similar to iodinated contrast material, which directly measures intravascular BF. ICG-VE has become popular in intraoperative BF monitoring, and two groups have recently compared transit-time flowmetry and ICG-VE during coronary bypass surgery.[17,18] However, it is still difficult to directly compare the results obtained using different techniques. One of the practical issues is that ICG-VE usually provides qualitative evaluation for vascular surgery, and another is the difficulty in identifying vessel structures as gray-scale images through the microscope eyepieces, without a simultaneous view of anatomical structures under natural light. Several groups have attempted to develop quantitative evaluation of circulation conditions after EC-IC bypass.[19,20] However, these studies were mainly focused on the peak time of ICG dynamics; therefore, the results were still only semi-quantitative. To overcome these issues, we developed FlowInsight for the quantitative analysis of ICG-VE and linked a wireless monitor to the operating microscope via a video switcher. Although the functions of FlowInsight are designed based on perfusion imaging and the dye dilution theory, the quantitative results still need to be validated by gold standard techniques, such as ultrasound flowmetry. ICG-VE reflects TDC of a purely intravascular tracer, it is therefore suitable for investigating vascular structures including arteries, veins, and bypass grafts on the brain surface. In our preliminary study, increased BF and shortened AT predicted postoperative hyperperfusion. Furthermore, we evaluated the graft BF by standardizing certain factors (e.g., ICG quantity, working distance, magnification, and kCBF). BF measurements and the prediction of hyper- or hypoperfusion are important practical issues in vascular surgery. Therefore, in the future, further studies with more patients are needed to identify appropriate parameters, to improve the data processing of ICG-VE.

From the practical point of view, real-time fusion of ICG-VE and natural light images by the video switcher provided simultaneous information on anatomy and circulation. It was possible to continue operating, manipulate vessels, and observe BF conditions projected on the wireless monitor. The monitor linked to the microscope shows BF and anatomical structures as well as the processed results of ICG-VE, electrophysiological monitoring, and neuronavigation. The monitor is designed for real-time transmission of HDMI signals and has dimensions of 130 × 55 × 43 mm with a weight of 145 g, small enough to have minimal impact on the operation of the microscope. Some recent microscopes have image overlay functions, which project information onto one of the eyepieces. However, this overlay function hides a part of the visual field in an eyepiece, and can disrupt stereoscopic viewing. By slightly changing the visual axes to the wireless monitor, we were able to obtain a range of image data without requiring movement of the head or body.

Real-time HGA mapping enabled rapid identification of areas of language and motor function. This procedure has a number of advantages. First, it is noninvasive. Second, it enables significant shortening of the time required for cortical mapping and detecting functional representations

for cortical regions hidden under the dura mater. Furthermore, it reduces the risk of seizure during awake craniotomies. In the present study, the ECoG analysis revealed characteristic HGA dynamics in the frontal and temporal language areas. One patient could understand the presented pictures, but could not name them aloud because of impairment of expressive language function. Although he had difficulties in the PN task during awake craniotomy, he slowly formed the names of the objects by moving his mouth. As a result, we observed a slight and slow HGA increase on MFG, following by a rapid HGA increase in the superior temporal region. These findings are valuable for understanding symptoms and the functional dynamics of human brains.

Although ECS is still the gold standard, it does carry a risk of seizures and requires adequate stimulus intensities. Sanai et al. proposed a new mapping procedure termed negative mapping.[21] According to their surgical experiences with 145 patients, they concluded that aggressive lesion resection could be safely achieved, without producing language deficits, because they did not find any positive language sites, even with limited cortical exposure. As a result, negative mapping is now widely accepted. Appropriate ECS is still indispensable for neurosurgeons despite the risk of seizure. Because our primary aim was to quickly perform brain mapping without using ECS, we focused on detecting neurophysiological signals directly from the brain surface. Thus, we observed motor- and language-related HGA on the brain surface and unexposed cortices by inserting electrode grids and strips. We believe that real-time HGA mapping is a viable alternative to negative mapping, and we expect that it will become the gold standard for identifying functional areas, which may finally remove the need for ECS.

In the present study, we focused on high-frequency oscillation because previous reports using chronic subdural grids stated that HGA accumulation indicated eloquent areas better than other frequency components. HGA shows strong correlations with various functional domains, including motor, auditory, visual, and language.[22–24] Roland et al. investigated two patients (one with a right-sided lesion and the other with a left-sided lesion) with ECoG recordings during awake craniotomy.[25] Although they used tongue movement and PN tasks, HGA mapping showed discrepancies with the results of ECS, especially for the PN task. In our study, the results of real-time HGA mapping clearly indicated the hand-motor and frontal language areas, which were validated by ECS.

Further verification with a larger sample size is needed to clarify variations in BF and functional distribution as well as to investigate inter-patient differences. We believe that the proposed real-time techniques have great potential for IOM in neurosurgery.

Conclusion

We demonstrated the clinical impact of real-time data processing of fluorescence imaging and electrical signal oscillations in the brain. Parameters of processed ICG-VG enabled the monitoring of circulatory conditions on the brain surface and predicted the risk of hyperperfusion. Real-time HGA mapping rapidly indicated the eloquent areas of motor and language function and significantly shortened the operation time of awake craniotomy. These techniques can make IOM more reliable, and enable us to formulate rational and objective operation strategies. Furthermore, real-time digital signal mapping sheds light on the underlying physiological mechanisms in the human brain.

Acknowledgments

This work was supported in part by a Grant-in-Aid for Scientific Research (B) No. 24390337 from 2012 to 2015 and a Grant-in-Aid for Exploratory Research No. 26670633 from 2014 to 2016 from the Ministry of Education, Culture, Sports, Science and Technology (MEXT), as well as the European Union FP7 Integrated Project VERE No. 257695 and the EU project ‘High Profile’ No. 269356. The authors are grateful for their support. The authors wish to thank Mr. Masato Mizukami, Mr. Masatoshi Honda, and Mr. Yuji Matsubara Leica Microsystems, Japan for their technical support.

Conflicts of Interest Disclosure

The authors report no conflict of interest concerning the materials or methods used in this study or the findings reported in this paper.

References

1) Hoor FT, Mook GA: A linear reflection densitometer for indocyanine green. *Cardiovasc Res* 3: 373–380, 1969
2) Raabe A, Beck J, Gerlach R, Zimmermann M, Seifert V: Near-infrared indocyanine green video angiography: a new method for intraoperative assessment of vascular flow. *Neurosurgery* 52(1): 132–139; discussion 139, 2003
3) Gorki H, Patel NC, Balacumaraswami L, Pillai JB, Subramanian VA: Laser fluorescence angiography

reveals perfusion defects in retrograde cardioplegia. *Perfusion* 26: 536–541, 2011
4) Waseda K, Ako J, Hasegawa T, Shimada Y, Ikeno F, Ishikawa T, Demura Y, Hatada K, Yock PG, Honda Y, Fitzgerald PJ, Takahashi M: Intraoperative fluorescence imaging system for on-site assessment of off-pump coronary artery bypass graft. *JACC Cardiovasc Imaging* 2: 604–612, 2009
5) Kamada K, Todo T, Masutani Y, Aoki S, Ino K, Morita A, Saito N: Visualization of the frontotemporal language fibers by tractography combined with functional magnetic resonance imaging and magnetoencephalography. *J Neurosurg* 106: 90–98, 2007
6) Rutten GJ, Ramsey NF, van Rijen PC, Noordmans HJ, van Veelen CW: Development of a functional magnetic resonance imaging protocol for intraoperative localization of critical temporoparietal language areas. *Ann Neurol* 51: 350–360, 2002
7) Crone NE, Hao L, Hart J, Boatman D, Lesser RP, Irizarry R, Gordon B: Electrocorticographic gamma activity during word production in spoken and sign language. *Neurology* 57: 2045–2053, 2001
8) Yuzawa M, Kawamura A, Matsui M: Clinical evaluation of indocyanine green video-angiography in the diagnosis of choroidal neovascular membrane associated with age-related macular degeneration. *Eur J Ophthalmol* 2: 115–121, 1992
9) Zhao P, Zheng M, Yue C, Luo Z, Gong P, Gao G, Sheng Z, Zheng C, Cai L: Improving drug accumulation and photothermal efficacy in tumor depending on size of ICG loaded lipid-polymer nanoparticles. *Biomaterials* 35(23): 6037–6046, 2014
10) Zierler K: Indicator dilution methods for measuring blood flow, volume, and other properties of biological systems: a brief history and memoir. *Ann Biomed Eng* 28: 836–848, 2000
11) Kudo K, Terae S, Katoh C, Oka M, Shiga T, Tamaki N, Miyasaka K: Quantitative cerebral blood flow measurement with dynamic perfusion CT using the vascular-pixel elimination method: comparison with H2(15)O positron emission tomography. *AJNR Am J Neuroradiol* 24: 419–426, 2003
12) Grüner JM, Paamand R, Højgaard L, Law I: Brain perfusion CT compared with15O-H2O-PET in healthy subjects. *EJNMMI Res* 1: 28, 2011
13) Hana T, Iwama J, Yokosako S, Yoshimura C, Arai N, Kuroi Y, Koseki H, Akiyama M, Hirota K, Ohbuchi H, Hagiwara S, Tani S, Sasahara A, Kasuya H: Sensitivity of CT perfusion for the diagnosis of cerebral infarction. *J Med Invest* 61(1–2): 41–45, 2014
14) Plass KG: A new ultrasonic flowmeter for intravascular application. *IEEE Trans Biomed Eng* 11: 154–156, 1964
15) Ortega-Palacios R, Moreno E, Leija L, Vera A: Validation of a transit time blood flow meter used for coronary bypass surgery. *Conf Proc IEEE Eng Med Biol Soc* 2010 178–181, 2010
16) Bosma J, Minnee RC, Erdogan D, Wisselink W, Vahl AC: Transit-time volume flow measurements in autogenous femorodistal bypass surgery for intraoperative quality control. *Vascular* 18: 344–349, 2010
17) Hatada A, Okamura Y, Kaneko M, Hisaoka T, Yamamoto S, Hiramatsu T, Nishimura Y: Comparison of the waveforms of transit-time flowmetry and intraoperative fluorescence imaging for assessing coronary artery bypass graft patency. *Gen Thorac Cardiovasc Surg* 59: 14–18, 2011
18) Balacumaraswami L, Abu-Omar Y, Choudhary B, Pigott D, Taggart DP: A comparison of transit-time flowmetry and intraoperative fluorescence imaging for assessing coronary artery bypass graft patency. *J Thorac Cardiovasc Surg* 130: 315–320, 2005
19) Uchino H, Nakamura T, Houkin K, Murata J, Saito H, Kuroda S: Semiquantitative analysis of indocyanine green videoangiography for cortical perfusion assessment in superficial temporal artery to middle cerebral artery anastomosis. *Acta Neurochir (Wien)* 155: 599–605, 2013
20) Horie N, Fukuda Y, Izumo T, Hayashi K, Suyama K, Nagata I: Indocyanine green videoangiography for assessment of postoperative hyperperfusion in moyamoya disease. *Acta Neurochir (Wien)* 156: 919–926, 2014
21) Sanai N, Mirzadeh Z, Berger MS: Functional outcome after language mapping for glioma resection. *N Engl J Med* 358: 18–27, 2008
22) Kunii N, Kamada K, Ota T, Greenblatt RE, Kawai K, Saito N: The dynamics of language-related high-gamma activity assessed on a spatially-normalized brain. *Clin Neurophysiol* 124: 91–100, 2013
23) Leuthardt EC, Miller K, Anderson NR, Schalk G, Dowling J, Miller J, Moran DW, Ojemann JG: Electrocorticographic frequency alteration mapping: a clinical technique for mapping the motor cortex. *Neurosurgery* 60(4 Suppl 2): 260–270; discussion 270–271, 2007
24) Sinai A, Bowers CW, Crainiceanu CM, Boatman D, Gordon B, Lesser RP, Lenz FA, Crone NE: Electrocorticographic high gamma activity versus electrical cortical stimulation mapping of naming. *Brain* 128(Pt 7): 1556–1570, 2005
25) Roland J, Brunner P, Johnston J, Schalk G, Leuthardt EC: Passive real-time identification of speech and motor cortex during an awake craniotomy. *Epilepsy Behav* 18(1–2): 123–128, 2010

Address reprint requests to: Kyousuke Kamada, MD, PhD, Department of Neurosurgery, Asahikawa Medical University, 2-1, Midorigaoka-Higashi, Asahikawa, Hokkaido 078-8510, Japan.
e-mail: kamady-k@umin.ac.jp